MECHANICAL PROPRIETIES OF PEELABLE COATINGS EMPLOYED FOR CBRN DECONTAMINATION

Daniela PULPEA[1], Bogdan Gheorghe PULPEA[2]*, Liviu MATACHE[3], Adrian ROTARIU[4], Toader GABRIELA[5], Traian ROTARIU[6], Florin DÎRLOMAN[7], Pamfil ȘOMOIAG[8], Alice PODARU[9], Mihai Ionuț UNGUREANU[10]

In this study, a PVA-based decontamination coating was subjected to mechanical investigations. The mathematical model employed for the numerical simulation of the polymeric coating behavior was chosen based on the results obtained by tensile and peeling experimental tests. According to research on four different types of polymeric coatings that differ based on the complexing agent, the chelator can affect both the mechanical properties and the decontamination factor. Given the experimental mechanical testing results, Ogden's law was shown to be the most appropriate technique to characterize the behavior of these viscoelastic peelable films. The results show that the numerical simulation accurately predicted the tensile and peeling test outcomes.

Keywords: polymeric coating, mechanical properties, peeling test, tensile test, numerical simulation

1. Introduction

The numerical simulation of polymeric materials [1] is based on their hyperelasticity or viscoelasticity. Even though the characterization of these coatings is quite complex for quasi-static problems, they can be considered incompressible materials such as rubber. LS-DYNA contains several models [2] that define the behavior of this class of materials, i.e., the material laws indicated by Blatz and Ko [3], Mooney [4] and Rivlin [5], Arruda and Boyce [6], Yeoh [7], Ogden [8] and Hill [9].

[1] Scientific Researcher, PhD Eng., Military Technical Academy, Bucharest, Romania, daniela.pulpea@mta.ro
[2] Lecturer, PhD Eng., Military Technical Academy, Bucharest, Romania, bogdan.pulpea@mta.ro; * corresponding author
[3] Scientific Researcher, PhD Eng., Military Technical Academy, Bucharest, Romania, liviu.matache@mta.ro
[4] Professor, PhD Eng., Military Technical Academy, Bucharest, Romania, adrian.rotariu@mta.ro
[5] Associate professor, PhD Eng., Military Technical Academy, Bucharest, Romania, gabriela.toader@mta.ro
[6] Professor, PhD Eng., Military Technical Academy, Bucharest, Romania, traian.rotariu@mta.ro
[7] PhD Student Eng., Military Technical Academy, Bucharest, Romania, florin.dirloman@mta.ro
[8] Professor, PhD Eng., Military Technical Academy, Bucharest, Romania, pamfil.somoiag@mta.ro
[9] PhD Student, Military Technical Academy, Bucharest, Romania / Faculty of Chemical Engineering and Biotechnologies, University 'Politehnica' of Bucharest, Romania, alice.podaru@mta.ro
[10] Eng., Military Technical Academy, Bucharest, Romania, mihai.ungureanu@mta.ro

The strain rate varies throughout the structure of the material, which is dictated by tensile forces or peeling forces. This factor must be considered when describing a polymeric material. The hyperelastic laws must include additional viscosity-related variables to account for the rate dependency. The large drawback to characterizing such materials is that so many criteria are necessary to be determined for each type of polymeric component.

Usually, the material identification parameters are quite complex and time-consuming. At the industrial level, the time available to produce the results by numerical simulation is limited. From the user's point of view, the most effective laws for describing the material are undoubtedly those based on the data of stress-strain curves obtained by practical testing. In this way, although processing the raw data is necessary, the adjustment operations required for the time-consuming analytical formulations can be avoided. It should be emphasized, however, that a predictive analysis based on experimental testing of materials is needed [10] [11].

This study describes the analyses performed to characterize Poly (vinyl alcohol)-based (PVA-based) coatings, evenly distributed by spraying or directly pouring it on the surfaces, used for surface decontaminating heavy metals and radioactive materials. The mechanical behavior of four polymeric films is assessed via less complex uniaxial tensile and peeling tests. Simulation of the uniaxial tensile test and the Ogden law is employed to determine the mechanical model parameters of the most promising tested coating. The same parameters, combined with additional options for the surface/coating interaction, are used to simulate the peeling test. The simulation results are similar to those obtained in real tests, showing that the proposed approach for the mechanical characterization of coatings, based on less complex mechanical tests and simulation tools, provides concluding and pertinent information.

2. Materials and methods

2.1. Materials

1.1. Polymeric coating: 10% PVA-based aqueous solution Poly(vinyl alcohol) (PVA with 98–99% hydrolysis degree, DP ≈ 1700-1800, Mw ≈ 115000 Da – Loba Chemie; Bentonite – Sigma–Aldrich; Anhydrous glycerol – Sigma–Aldrich; chelating agents – solution 1 (S1) with EDTA: Ethylenediaminetetraacetic acid, tetrasodium salt dihydrate, PBTC:2-Phosphonobutane-1,2,4-tricarboxylic acid, Catechol:1,2-dihydroxybenzene and IDS:Iminodisuccinic acid); Surface: glass plates (120x120mm) and galvanized metal plates (100x30 mm).

The decontamination solutions were poured into 120x120mm glass moulds and 100x30 mm metal plates and allowed to solidify until the solvent completely evaporated and the coatings were detached from the surfaces.

2.2. Methods

The nano-clay was added after the complexing agent has been dissolved in distilled water. For 24 hours, the clay was vigorously stirred at room temperature to ensure thorough dispersion and hydration. The following procedure involved adding the polymer gradually and dissolving it completely while stirring (at a speed of 500 rpm) for 4 hours at 100°C. The plasticizer was added last, followed by final stirring at room temperature for another 30 minutes. Four decontamination solutions, which differ from each other depending on the complexing agent, were prepared following this procedure: S1 with EDTA, S2 with PBTC, S3 with Catechol, and S4 with IDS.

The test program was established based on how the decontamination coatings are used, and especially how they are removed by peeling. Following the solution casting on a contaminated surface, the water content evaporates, producing a coating. This film must have good contact with the surface, but at the same time, the adhesion needs to be reduced because it is necessary to remove the film using a lower force. Thus, an optimal balance must be maintained between allowing easy coating removal and adequate adhesion to achieve effective decontamination.

However, using only the peeling test does not provide the data necessary to build the model of the mechanical behavior of the coatings. Given that the loading parameters encountered in practice are highly varied, more or less complex tests are required for such an objective. In our approach, we started from the idea that the uniaxial tensile test provides enough data to characterize the behavior of the coating when the peeling is happening.

2.2.1. Tensile test

The uniaxial loading test on polymer films allows the investigation of their basic mechanical properties regarding stress (σ) vs. strain (ε). The tensile testing was performed by applying an increasing axial force on a sample, and both axial force and the elongation of the test specimen were recorded. In carrying out these tests ISO 37: 2011(E) standard was used as a reference [12]. The standard describes a method for determining the properties such as stress and specific deformation for vulcanized rubbers and thermoplastics. There are two acceptable shapes, one like a dumbbell and the other like a ring. Dumbbell-shaped specimens were employed in this study, and Table 1 and Fig.1 below provide geometry information.

Since, in this case, the tensile strength (σ) is the same as the breaking strength, the maximum stress was calculated using the following equation:

$$\sigma = \frac{F_m}{W \times t} \ (MPa) \tag{1}$$

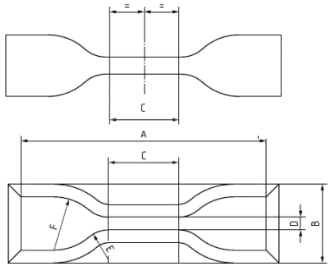

Fig. 1. Tensile test sample geometry [12]

Table 1

Specimen measurement

Dimensions	Unit (mm)
A Overall length	75
B Width of ends	12.5±1.0
C Length of narrow portion	25.0±1.0
D Width of narrow portion	4.5±0.1
E Transition radius outside	8.0±0.5
F Transition radius inside	10.5±1.0

where: Fm = maximum force recorded – axial force, (N); W = average width of the narrow part of the punching knife, (mm); t = sample thickness, (mm).

The specific strain (ε) produced by the tensile force on the material was calculated using the following equation:

$$\varepsilon = \frac{100\times(L_r - L_0)}{L_0}(\%) \quad (2)$$

where: Lr = length at breaking point, (mm); Lo = initial length, (mm).

Testing was conducted on 4 decontamination solutions that vary in terms of the complexing agent (S1 with EDTA, S2 with PBTC, S3 with Catechol, and S4 with IDS). From each type of material, 5 specimens were cut to be tested. The samples were fixed in the clamps of the tensile testing machine. The variation in elongation and force was continuously recorded with an accuracy of ±0.2% at a testing speed of 8.33 mm/s (200 mm/mm).

2.2.2. Peeling test

The peeling test is the most common method for measuring surface adhesion and can be performed in several ways depending on the angle variation and the type of testing device. The most common tests are the 180° angle peeling test and "T-peel" at 90°. Removing decontamination films from surfaces can pose several problems at once. Thus the force required to remove the films varies with the speed and angle at which they are removed.

The films were prepared by casting 10 g of each of the four solutions (S1, S2, S3, S4) onto 100x30 mm molds, ensuring a film thickness of 0.5 mm after solvent evaporation. The peeling surface was a galvanized metal plate with a roughness that guaranteed a better adhesion of the coating. Previously peeling tests were done on glass, mirror-finished stainless steel plates, and ceramics, and the forces were too weak to be recorded, or the film dethatched by itself from the surface after it was formed. The 180° peel test was performed following the Standard Test Method for Pressure Sensitive Adhesive Tape [13] for determining the peel strength or bond strength between two surfaces using the universal testing machine mechanics type ZMGi500 to which the S2M (0...20N) force transducer was connected. The metal plate was fixed at the bottom of the machine (in the movable part), and the film was attached, by an extension of material made of

adhesive tape, to the top of the machine (in the fixed part) where the force transducer is placed. A schematic illustration of the setup at various points during the testing period is shown in Fig.2. This testing aimed to determine the minimum force required to peel the decontamination coatings from a surface. The variation of force as a displacement function over an angle of 180° was observed and recorded with an accuracy of ±0.02% for a constant test speed of 3.11 mm/s (60 mm/min), and 3 tests were carried out for each type of film.

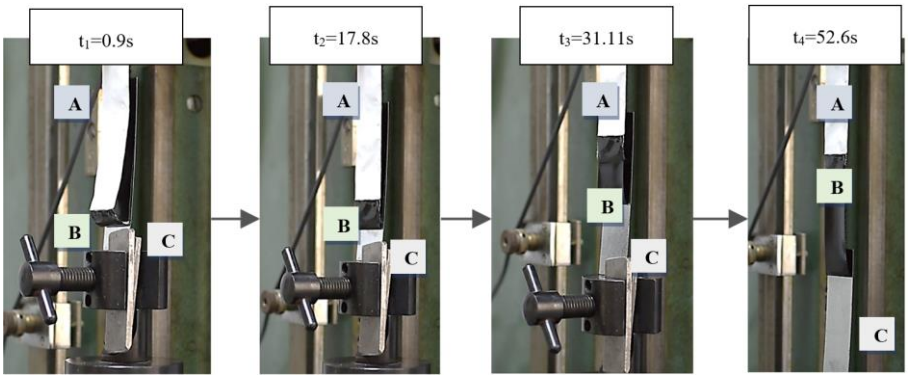

Fig. 2. Peeling test steps exemplification
A: upper white film – adhesive tape used as an extension of the polymer film,
B: black film – polymer film to be tested, C: lower white film – metal support assumed to be contaminated

2.2.3. Numerical simulation

Ogden's law [8] was considered for the simulation of the tensile and peeling tests, which determines the mathematical model of the material since these equations best defined the practically obtained film characteristics. Since the shear modulus is significantly smaller than the elasticity modulus, rubber-like materials are typically considered incompressible. A convolution integral with strain energy functional in terms of relative volume is introducing a hydrostatic term for the mathematical modeling of rubber, according to J. Ogden [14]:

$$W^* = \sum_{i=1}^{3} \sum_{j=1}^{n} \frac{\mu_j}{\alpha_j} \left(\lambda_i^{*\alpha_j} - 1 \right) + K(J - 1 - lnJ) \quad (3)$$

where * indicates that the volumetric effects have been removed from the main stretches, λi; n – can vary between 1 and 8 inclusive; K – is the bulk modulus.

Strain rate effects are accounted for in linear viscoelasticity by form integral convolution:

$$\sigma_{ij} = \int_0^t g_{ijkl}(t - \tau) \frac{\partial_{\varepsilon kl}}{\partial_\tau} d\tau \quad (4)$$

or in terms of the second Piola-Kirchhoff stress tensor and the strain tensor given by Green:

$$S_{ij} = \int_0^t G_{ijkl}(t - \tau) \frac{\partial_{\varepsilon kl}}{\partial_\tau} d\tau \quad (5)$$

where g_{ijkl} and G_{ijkl} are the relaxation function of the material for different stress measurements.

For the tensile test sample, the equivalent model was discretized using a number of 7200 hexahedral elements and a number of 11325 nodes. The elements are of type 3 hexahedral with 8 nodes, with integration at all nodes that also allow nodal rotations. Fig. 3 shows the dimensions and discretization of the films for the mathematical analysis of the tensile test.

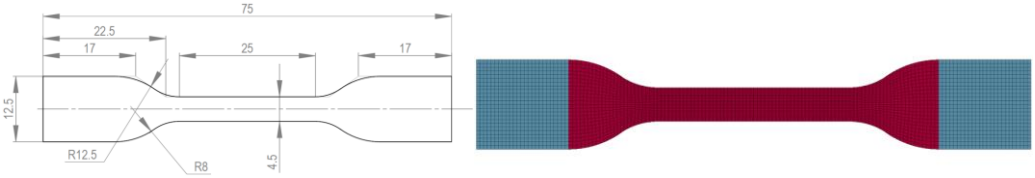

Fig. 3. Physical and discretization model of tensile test specimens

The same kind of elements was used for the peeling test samples, but while discretizing the analogous model, 2600 hexahedral elements and 4356 nodes were applied. Fig.4 illustrates the size and discretization of the films used in the mathematical analysis of the peeling test.

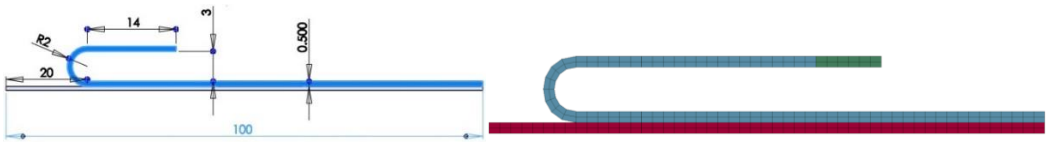

Fig. 4. Physical and discretization model of peeling test specimens

The constants of material models introduced in the calculation by numerical simulation are presented in Table 2.

Table 2

Material parameters

					MID – Material identification number
MID	RO	PR	N	NV	RO – Mass density
					PR – Poisson ratio
1	11.284E-9	0.49	3	3	N – material-adjusted Ogden model constant
					NV – Prony series number - material constant
					SGL – sample length
SGL	SW	ST	LCID1	DATA	SW – sample width
					ST – sample thickness
25	4.56	0.54	9	1	LCID1 – force curve versus material displacement
					DATA – default uniaxial data

The peeling test was investigated on a length significantly shorter than the original one of 80 mm to decrease the amount of time required to simulate the

process. Additionally, several characteristics that describe how the material interacts with the surface were used in the simulation, including:

Table 3

Tiebreak node to surface parameters

				NFLF – Normal breaking force - default
NFLF	SFLF	NEN	MES	SFLF – elongation at break
				NEN – normal force exponent - default
1	0.2	1	1	MES – elongation exponent - default

3. Results and discussions

The behavior of the decontamination films under static mechanical tensile stress was investigated. The maximum tensile force (Fm) values and the maximum elongation before breaking were reported. These data were used to calculate the stress and effort further, and corresponding graphs were created.

Fig.5 shows how the samples appeared both before and after the mechanical tensile testing. However, even if the material tends to return to its previous shape, this is still not possible since it is partially affected by undergoing mechanical testing.

Fig. 5. Sample appearance before and after tensile testing

The average thickness value (tm), determined at three points along the length of the specimen (at the center C, and at each end: E1, E2) was used to calculate stress and strain. After subjecting of the films to uniaxial stretching stress, Table 4 shows all the values obtained by measuring, recorded by the testing machine, and calculated using the formulas shown above.

The calculated specific stress and strain were plotted on graphs for each of the five samples of each type of material. Maximum values for σ and ε showed in Table 4 give information on the behavior of the material and for data interpretation.

Table 4

Tensile test resulting values

Name / Specimen no		Dimensions						Recorded values		Calculated values	
		E1	C	E2	t_m (mm)	W (mm)	S0 (mm^2)	F_m (N)	L_r (mm)	σ (MPa)	ε (%)
S1	1.1	0.68	0.677	0.707	0.69	4.5	3.11	68.0	243.32	21.9	386.6
	1.2	0.825	0.904	0.938	0.89	4.5	4.01	73.9	238.25	18.45	376.5
	1.3	0.868	0.94	0.958	0.92	4.5	4.14	80.8	246.55	19.52	393.1
	1.4	0.997	0.92	0.856	0.92	4.5	4.14	82.6	245.23	19.95	390.5
	1.5	0.923	0.963	0.99	0.96	4.5	4.32	89.7	243.90	20.76	387.8
S2	2.1	0.64	0.578	0.605	0.61	4.55	2.78	22.5	145.94	8.10	191.9
	2.2	0.951	0.955	0.928	0.94	4.55	4.28	79.1	268.00	18.49	436.0
	2.3	1.054	1.155	1.125	1.11	4.55	5.05	73.0	241.32	14.45	382.6
	2.4	1.186	1.155	1.2	1.18	4.55	5.37	78.0	251.12	14.53	402.2
	2.5	1.253	1.242	1.23	1.24	4.55	5.64	65.7	223.46	11.64	346.9
S3	3.1	0.527	0.534	0.545	0.54	4.56	2.46	54.1	291.59	21.97	483.2
	3.2	0.818	0.8	0.751	0.79	4.56	3.60	78.6	285.95	21.82	471.9
	3.3	0.86	0.885	0.936	0.89	4.56	4.06	95.5	296.91	23.53	493.8
	3.4	1.00	0.954	1.022	0.99	4.56	4.51	79.4	232.11	17.59	364.2
	3.5	0.877	1.047	1.064	1.00	4.56	4.56	82.4	257.78	18.07	415.6
S4	4.1	0.533	0.475	0.521	0.51	4.55	2.32	48.5	236.17	20.90	372.3
	4.2	0.95	0.968	0.95	0.96	4.55	4.37	98.1	239.91	22.46	379.8
	4.3	1.082	1.096	1.091	1.09	4.55	4.96	97.5	222.05	19.66	344.1
	4.4	1.07	1.12	1.131	1.11	4.55	5.05	97.8	227.69	19.36	355.4
	4.5	1.07	1.096	1.092	1.09	4.55	4.96	87.8	216.64	17.70	333.3

The force versus strain is represented in Fig.6. To be able to compare the tested samples graphically, it was decided to define a measuring unit similar to engineering stress, which is defined as the ratio between the recorded force, F, and the initially measured surface, S0, shown in table 4. This was done since the forces varied greatly between specimens because their specific thickness could not be kept constant during film formation.

In Fig.6 it is illustrated that the materials can be stretched at a constant speed with a force up to five times its initial length before breaking. Therefore, under tensile testing conditions, the samples can be categorized as hyperelastic materials that allow very large deformations. The response of a polymeric material to external stress is closely related to temperature, applied stress, and the test speed. During tensile testing, the temperature was not varied, so it is not a factor that interferes with the response given by the material after the test. To highlight the hyperelasticity of the materials, comparative tests were made, and the Stress/Strain graphs are shown in Fig.7. As a result, it can be observed that all the peelable coatings that were tested have a viscoelastic character similar to that of rubber [11] and with very high elongation as the stress increases at a constant speed.

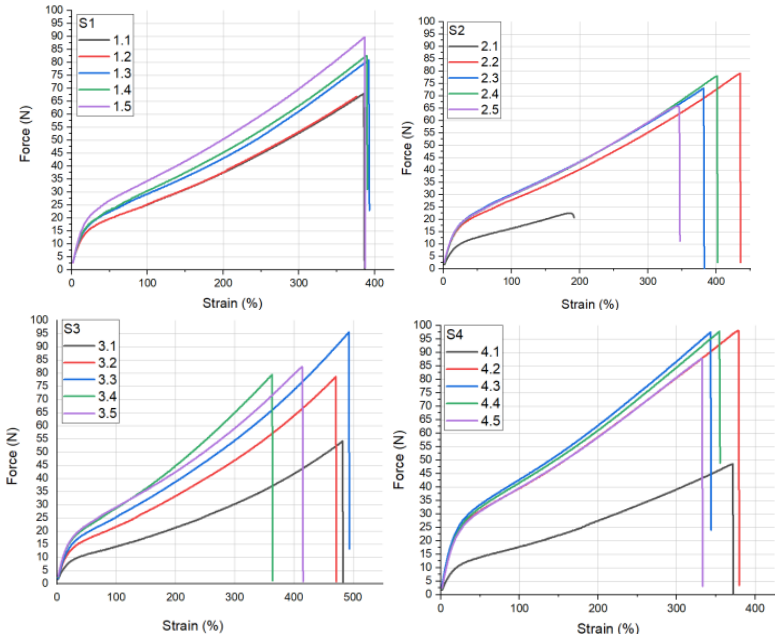

Fig.6. Decontamination coatings schematic representation of force and strain curves

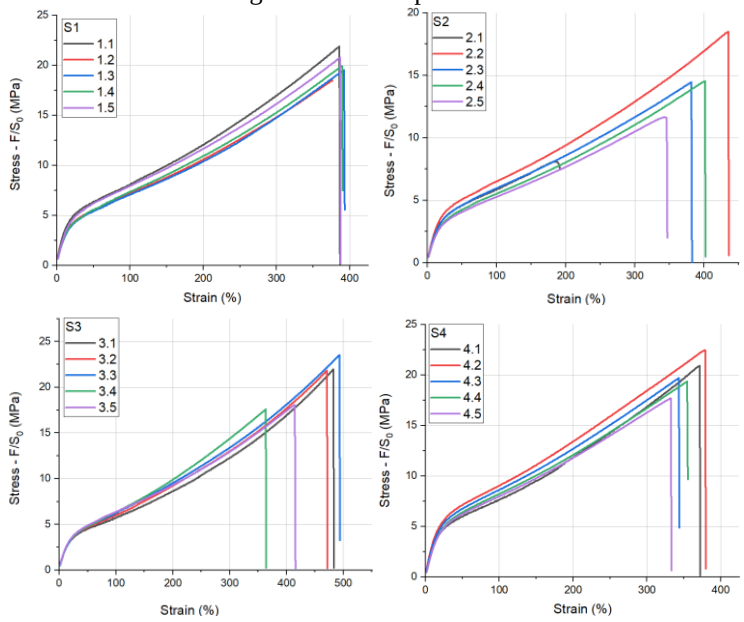

Fig. 7. Decontamination coatings schematic representation of stress and strain curves

In the tensile test presented above the average values were as follows: σ=20.08 ± 0.63MPa and ε=390.45 ± 2.65% for S1, σ=13.54 ± 1.64MPa and ε=377.26 ± 28.04% for S2, σ=20.62 ± 2.2MPa and ε=456.88 ± 36.21% for S3 and σ=19.97 ± 0.81MPa and ε=357.27 ± 14.19% for S4. The values obtained from the tensile tests of S3 peelable coating were employed in numerical simulations since it generated the best results.

The peeling test aimed to determine the minimum force required to strip the decontamination coatings from a galvanized metal sheet at an angle of 180°. Additionally, the surface adherence and peeling behavior of the polymer films were studied. This conduct is visually described in Fig.8, which represents the film peeling of at various test times. The highest value for the peeling force of 0.6-1.2 N was recorded for the S3 coating, as can also be seen in Fig.8. Thus, it can be confirmed that this film had superior surface adhesion among of all the tested films. To strip S1 coating from the surface a 0.1-0.6 N force was required, 0.1-0.3 N for S4 and for S2 the force was below the detection limit of the sensor. Through peeling tests, the behavior of the films at the moment of detachment from metal surfaces was investigated by applying a load with a constant speed until the moment of their total separation from the surface and determining the minimum force necessary for their detachment.

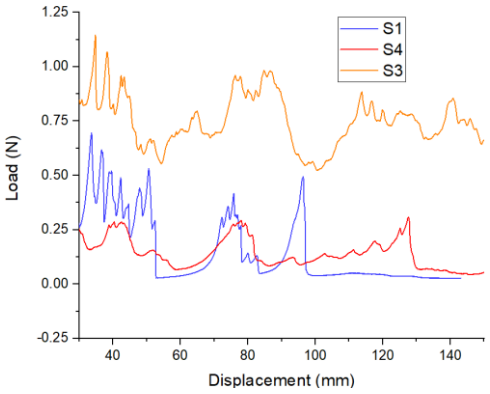

Fig. 8. Peeling test resulting graphs of load versus displacement

Fig. 9 and Fig. 10 illustrate the mathematical model results for the simulation of the tensile test and peeling of the S3 polymeric coating. By analyzing all the images that represent the mathematical model of the tensile test, it is possible to see how the deformation of the material takes place over time. Through numerical simulation, the formulation of a theoretical model was aimed that is in accordance with the experimental data. Based on the reference data, it was determined that numerical simulation utilizing Ogden's laws to define such a material is the optimum method that can be applied to mathematical models for viscoelastic materials. Through practical tests and mathematical modeling, it is confirmed that the coating is a viscoelastic material that could be characterized including through numerical simulation. The method used for the simulation was an implicit one in which the user sets the integration step, due to the fact that an explicit analysis of the phenomenon is time-consuming.

In the previous section, the data collected by the tensile and peeling test machines were represented graphically. In Fig.11, the experimental data are plotted in comparison to numerical simulation data of mathematical modeling. In this method, a good similarity between the calculated force estimations and the force

values measured experimentally can be observed. This illustrates the validity of the developed mathematical model, which will be able to predict the factors that may cause the breaking of polymer films and their separation from surfaces in the future.

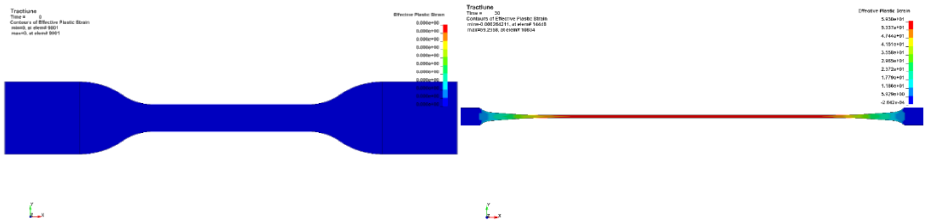

Fig.9. Tensile test mathematical simulation

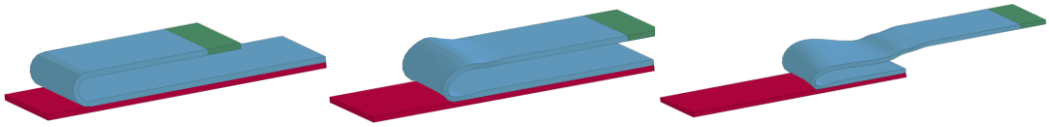

Fig.10. Peeling test mathematical simulation

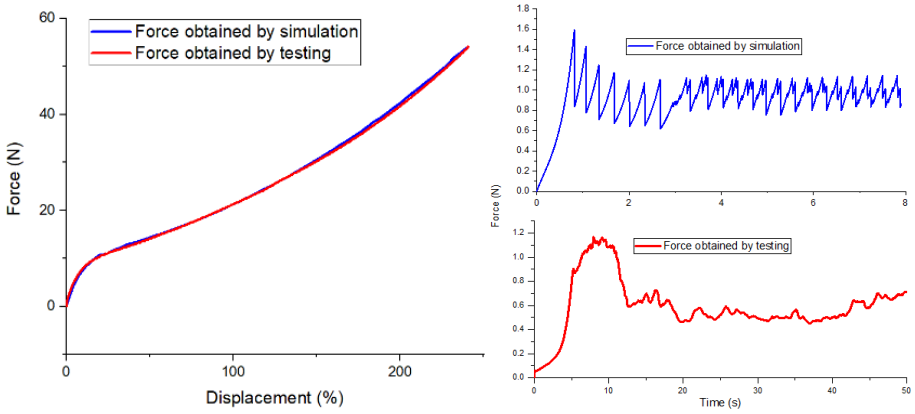

Fig. 11. Peeling force versus peeling displacement comparison plot

4. Conclusions

The behavior of the decontamination films under static mechanical tensile stress was determined in accordance with international standards by applying a load with a constant speed of 8.33 mm/s at a temperature of 20°C until breaking point. Five samples were synthesized and tested for each type of film. The values of the maximum tensile force and the maximum elongation before breaking were reported. The behavior of the films at the moment of detachment from metal surfaces was determined by applying a force with a constant speed of 3.11 mm/s until the moment of their total separation from the surface, and the determination of the minimum force necessary for their detachment was calculated. For each kind of material, 3 samples were prepared and put to the test, under ASTM D3330 conditions. The mechanic proprieties, such as stress and strain, were calculated and plotted based on these measurements. The deformation of the films at a constant

rate of stress is very high, as is characteristic of hyperelastic materials. Based on the outcomes of the tensile and peeling tests, it was observed that S3 polymeric coating performed better than the other coatings in these conditions.

The numerical simulation of the tension and peeling tests was carried out to provide a set of Ogden model parameters to describe the mechanical behavior of the decontamination coating. The proposed approach for the coating's mechanical characterization is viable, even if it is based on less complex mechanical tests and simulation tools, as long as the simulation results are similar to those obtained in real tests.

Acknowledgments

This work was financially granted by the Ministry of Research, Innovation, and Digitalisation (UEFISCDI) through ctr.no.PD 69/2022 and ctr.no.672PED/2022. Alice Podaru gratefully acknowledges the financial support from the European Social Fund from the Sectoral Operational Programme Human Capital 2014-2020, through the Financial Agreement with the title "Training of Ph.D. students and postdoctoral researchers to acquire applied research skills - SMART", Contract no. 13530/16.06.2022 - SMIS code: 153734

R E F E R E N C E S

[1] *Brinson H and Brinson L.* Polymer engineering science and viscoelasticity: an introduction. Evanston: Springer Verlag, 2008.
[2] LS-DYNA User-Manual and Theoretical Manual, Livermore Software Technology Corporation
[3] *Blatz P.J, Ko W.L.*, Application of finite elastic theory to the deformation of rubbery materials, Transaction of the Society of Rheology, 6, 223-251, 1962.
[4] *Mooney M*., A theorie of elastic deformation, Journal of Applied Physics, 11, 582-593, 1940.
[5] *Rivlin R.S.*, Large elastic deformation of isotropic materials. Fundamental concepts, Philosophical Transactions of the Royal Society of London, Seies A 240, 459-490, 1948.
[6] *Arruda E. M., Boyce M.C.*, A three-dimensional constitutive model for the large stretch behacior of rubber elastic materials, J. Mech. Phys. Solids, Vol. 41, 389-412, 1993
[7] *Yeoh O.H*., Characterisation of elastic proprieties of carbon-black-filled rubber vulcanisates, Rubber Chemistry and Technology, 63, 792-805, 1990.
[8] *Ogden R.W.,* Elastic deformation of rubber-like solids mechanics of solids, Mechanics of Solids, In: Hopkins, H.H, Sewell, M.J (eds); The Rodney Hill 60th Anniversary volume, Pergamon Press, Oxford, 1982.
[9] *Hil R.,* Aspect of invariance in solid mechanics, Adv. Appl. Mech., 18, 1-75, 1978.
[10] *Benson D.J., Kolling S., Du Bois P.A*., A simplified approach for strain-rate depedent hyperelastic materials with damage, 9th International LS-DYNA Users Conference – Material Modeling, 1-14, 2016.
[11] *Majid Shahzad, Ali Kamran, Muhammad Zeeshan Siddqui, Muhammad Farhan*, Mechanical characterization and FE modelling of a hyperelastic material, Materials Research, 918-924, 2015.
[12] ISO 37:2011(en) Rubber, vulcanized or thermoplastic — Determination of tensile stress-strain properties
[13] Standard Test Method for Peel Adhesion of Pressure-Sensitive Tape, ASTM INTERNATIONAL, D3330/D3330M-04, 2018
[14] *Ogden R. W.*, Non-linear elastic deformation, ZAMM-Journal of Applied Mathematics and Mechanics, 65(9), John Wiley& Sons Ltd., 1985.